JOURNAL OF SOLID STATE CHEMISTRY 58, 221–225 (1985)

# The Structure and Magnetic Properties of Chromium(III) Molybdate

P. D. BATTLE,* A. K. CHEETHAM,† W. T. A. HARRISON, AND N. J. POLLARD

*Inorganic Chemistry and Chemical Crystallography Laboratories, South Parks Road, Oxford OX1 3QR, England*

AND J. FABER, JR.

*Materials Science and Technology Division, Argonne National Laboratory, Argonne, Illinois 60439*

Received August 29, 1984; in revised form December 4, 1984

Magnetic susceptibility measurements have shown that $Cr_2(MoO_4)_3$ orders magnetically at 42 K. Powder neutron diffraction experiments at 295 and 5 K indicate that $Cr_2(MoO_4)_3$ is chemically and magnetically isostructural with the L-type ferrimagnet $Fe_2(MoO_4)_3$, and has a magnetic moment of 2.5 $\pm$ 0.2 $\mu_B$ per cation at 5 K. The limitations imposed on powder neutron diffraction methods by particle-size effects are discussed. © 1985 Academic Press, Inc.

## Introduction

The magnetic and electrical properties of transition metal salts with garnet-related structures have been extensively studied. Recent work has focused on the interactions between the three different sublattices ($A$, $M$, and $X$) which occur in the mineral as represented by the formula $A_3M_2(XO_4)_3$. Our own work (*1, 2*) has included studies of the L-type ferrimagnets $Fe_2(SO_4)_3$ and $Fe_2(MoO_4)_3$ where the dodecahedral $A$ sites are vacant, the tetrahedral $X$ sites are diamagnetic, and only the octahedral $M$ sites are occupied by magnetic ions. The magnetic ordering in these two compounds is essentially antiferromagnetic, but a weak ferrimagnetism arises because, although the $FeO_6$ octahedra are very similar, there is more than one crystallographic $Fe^{3+}$ site in the structure and the different sites exhibit slightly different magnetizations at low temperatures (*3*). The magnetic superexchange takes place along pathways of the form Fe–O–X–O–Fe and leads to Curie temperatures of 28 and 12 K in the sulfate and molybdate, respectively. The factors that determine these temperatures are thought to include the electronegativity of $X$ (*2*) and the length of the superexchange pathway, a detailed analysis of the lengths of the chemical bonds in $Fe_2(SO_4)_3$ having suggested that the strength of the magnetic interaction varies inversely as the 36th power of the length of the superexchange pathway (*4*).

To monitor the effects of cation size and $d$-orbital occupation number on the mag-

* Permanent address: Dept. of Inorganic and Structural Chemistry, Leeds University, Leeds, LS2 9JT, England.

† To whom correspondence should be addressed.



0022-4596/85 $3.00

netic behavior of this type of structure, we have extended our studies to include chromium molybdate, $Cr_2(MoO_4)_3$. The decrease in ionic radius on moving from $Fe^{3+}$ to $Cr^{3+}$ might be expected to cause an increase in the Curie temperature but the change from half-filled $e_g$ orbitals to empty $e_g$ orbitals will eliminate the $\sigma$ superexchange interactions and may lead to the adoption of a completely different spin arrangement in the magnetically ordered phase. In order to determine whether the $\pi$ superexchange in these systems is strong enough to produce magnetic ordering and, if so, at what temperature and with what spin arrangement, we have performed magnetic susceptibility and neutron diffraction experiments on $Cr_2(MoO_4)_3$.

## Experimental

A polycrystalline sample of $Cr_2(MoO_4)_3$ was prepared as follows: 11.34 g of $Cr(NO_3)_3 \cdot 9H_2O$ and 7.5 g of $(NH_4)_6Mo_7O_{24} \cdot 4H_2O$ were each dissolved in 100 $cm^3$ of water. Citric acid (10 g) was added to the chromium nitrate solution which was then mixed with the ammonium heptamolybdate solution (*5*). The mixture was heated to dryness, giving an amorphous solid which formed crystalline $Cr_2(MoO_4)_3$ after annealing at 700°C for 48 hr. The sample was finally annealed at 300°C for a further 48 hr. Analytical electron microscopy (*6*) and atomic absorption analysis indicated that the product was a homogenous, single phase containing 17.5% Cr (calcd for $Cr_2(MoO_4)_3$ 17.8%). The magnetic susceptibility of the product was measured in the temperature range 4 K $< T <$ 80 K using an Oxford Instruments Faraday Balance operating with a main field of 9.95 kG and a field gradient of 122 G $cm^{-1}$. Room temperature time-of-flight powder neutron diffraction data were collected on the General Purpose Powder Diffractometer at the Intense Pulsed Neutron Source (IPNS), Argonne. All subsequent structure refinements were performed on the data collected at $2\theta = 90°$ with a channel width of 8 $\mu$s in order to achieve the optimum balance between counting statistics and resolution. Constant-wavelength ($\lambda = 2.988$ Å) neutron diffraction data were collected at temperatures of 5 and 295 K using the D1A diffractometer at ILL Grenoble, operating with a $2\theta$-step size of 0.05°. All of the neutron scattering experiments ran for 24 hr.

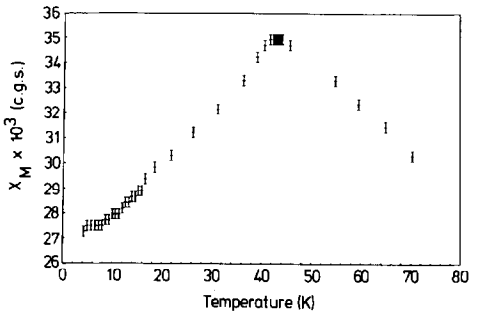


FIG. 1. The molar magnetic susceptibility of $Cr_2(MoO_4)_3$ as a function of temperature.

## Results

The molar magnetic susceptibility of $Cr_2(MoO_4)_3$ is plotted as a function of temperature in Fig. 1. It is apparent that the material orders magnetically at 42 K.

The room temperature neutron diffraction data were analyzed using a version of the Rietveld profile analysis program (*7*) modified to treat time-of-flight data (*8*). The X-ray powder diffraction pattern of our sample indicated that it was isostructural with the monoclinic phase of $Fe_2(MoO_4)_3$, a result which is consistent with Sleight and Brixner's earlier work (*9*), and we therefore used the atomic coordinates reported by Chen (*10*) for $Fe_2(MoO_4)_3$ as the starting point for our structure refinement. There are thus 34 atoms in the asymmetric unit in the space group $P2_1/c$. The temperature factors were fixed: $B_{Cr} = B_{Mo} = 0.6$, $B_O = 1.0$ (Å$^2$). Least-squares refinement led to the following values for the unit-cell parameters: $a = 15.569(3)$, $b = 9.1707(4)$, $c = 18.141(4)$, $\beta = 125.39(1)$. Figure 2 shows

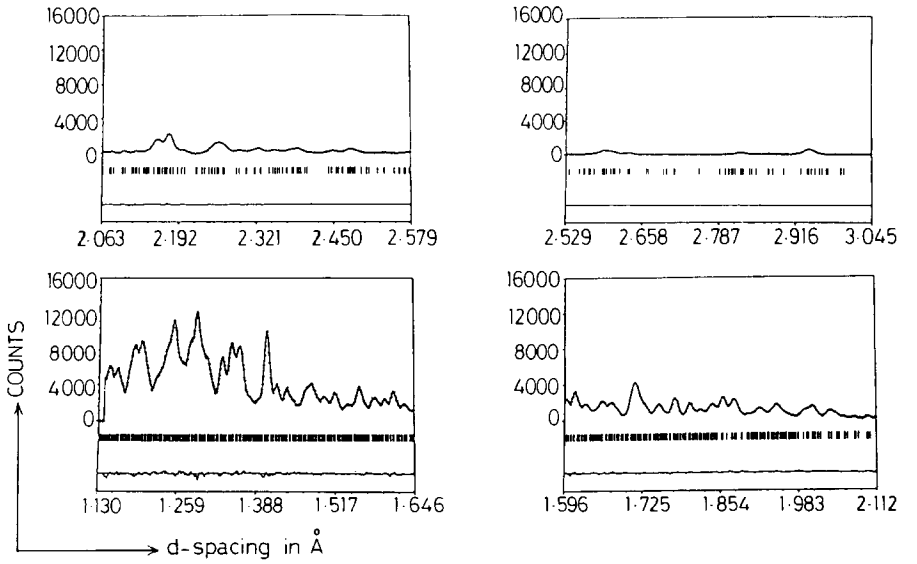


FIG. 2. The observed (+), calculated (−), and difference time-of-flight neutron diffraction patterns of $Cr_2(MoO_4)_3$ at room temperature.

the observed and calculated diffraction patterns after the refinement of 113 atomic and profile parameters using ~1800 profile points spread over ~1400 reflections. The agreement is very good ($R_{wpr}$ = 2.5%), but the standard deviations on the final atomic coordinates (Table I) are large, leading to standard deviations of ~0.1 Å in the metal-to-oxygen bond lengths (Table II). An attempt to refine the structure using the room temperature, constant-wavelength data gave similarly imprecise results. It appears that the problem is underdetermined and, although our analysis firmly establishes the general features of the $Cr_2(MoO_4)_3$ structure, a detailed crystallographic study will not be possible until a single crystal suitable for X-ray work can be prepared. The lack of data in the powder experiment is accentuated in this case because the preparative technique used to make the sample results in a rather small crystallite size, causing a broadening of the diffraction peaks which is reflected in the peak shape parameters. Our attempts to use a solid-state synthesis following the method of Sleight and Brixner (*9*) were unsuccessful.

As a consequence of the onset of magnetic ordering at 42 K the diffraction pattern observed at 5 K showed many changes from that recorded at room temperature (Fig. 3); for example, there is an increase in

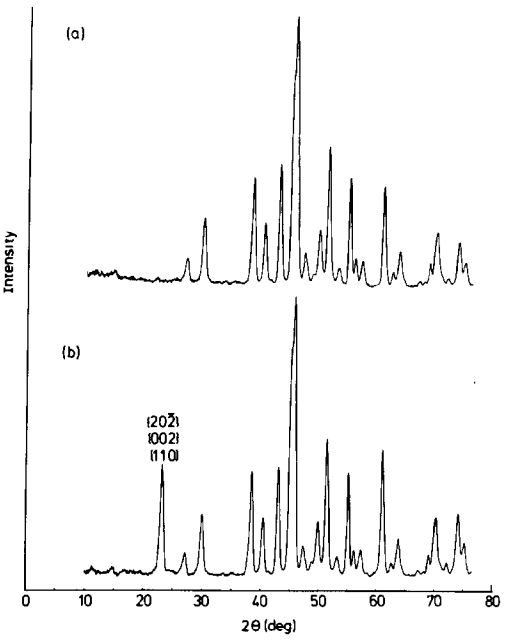


FIG. 3. The low-angle, constant-wavelength neutron diffraction pattern of $Cr_2(MoO_4)_3$ observed at (a) room temperature and (b) 5 K.

TABLE I

FINAL ATOMIC COORDINATES OF $Cr_2(MoO_4)_3$ AT ROOM TEMPERATURE

| | x | y | z |
|---|---|---|---|
| Cr 1 | 0.381(3) | 0.960(4) | 0.315(3) |
| Cr 2 | 0.378(4) | 0.451(4) | 0.047(3) |
| Cr 3 | 0.116(3) | 0.477(4) | 0.176(2) |
| Cr 4 | 0.108(3) | 0.999(4) | 0.417(2) |
| Mo 1 | 0.005(2) | 0.256(3) | 0.493(1) |
| Mo 2 | 0.361(1) | 0.123(2) | 0.138(1) |
| Mo 3 | 0.141(1) | 0.112(2) | 0.250(1) |
| Mo 4 | 0.152(1) | 0.624(2) | 0.380(1) |
| Mo 5 | 0.351(1) | 0.630(3) | 0.215(1) |
| Mo 6 | 0.001(1) | 0.733(3) | 0.021(1) |
| O 1 | 0.581(2) | 0.390(3) | −0.007(1) |
| O 2 | 0.988(2) | 0.413(2) | 0.171(2) |
| O 3 | 0.834(2) | 0.200(3) | 0.099(2) |
| O 4 | 0.768(2) | 0.509(3) | 0.047(2) |
| O 5 | 0.524(2) | 0.417(3) | 0.143(1) |
| O 6 | 0.739(2) | 0.515(2) | 0.282(1) |
| O 7 | 0.417(2) | 0.111(2) | 0.407(1) |
| O 8 | 0.181(1) | 0.293(3) | 0.247(1) |
| O 9 | 0.554(2) | 0.357(2) | 0.452(1) |
| O 10 | 0.393(2) | 0.320(2) | 0.982(1) |
| O 11 | 0.071(1) | 0.373(2) | 0.072(1) |
| O 12 | 0.415(2) | 0.343(2) | 0.509(1) |
| O 13 | 0.854(1) | 0.391(2) | 0.229(1) |
| O 14 | 0.257(1) | 0.030(2) | 0.516(1) |
| O 15 | 0.117(2) | 0.114(3) | 0.332(1) |
| O 16 | 0.531(2) | 0.941(3) | 0.360(1) |
| O 17 | 0.751(2) | 0.964(2) | 0.198(2) |
| O 18 | 0.670(2) | 0.928(2) | 0.298(2) |
| O 19 | 0.967(2) | 0.940(3) | 0.315(1) |
| O 20 | 0.097(2) | 0.314(3) | 0.592(1) |
| O 21 | 0.162(2) | 0.811(3) | 0.393(1) |
| O 22 | 0.047(2) | 0.660(2) | 0.122(2) |
| O 23 | 0.351(2) | 0.607(2) | 0.114(1) |
| O 24 | 0.345(1) | 0.816(2) | 0.225(1) |

the scattered intensity at $2\theta \sim 22°$, 38°, 61°, 74°. The large increases in the intensities of the {110}, {002}, and {20$\bar{2}$} reflections indicate that $Cr_2(MoO_4)_3$ has the same magnetic structure as $Fe_2(MoO_4)_3$ (*2*). In order to confirm this, the low-temperature data were analyzed by the Rietveld technique, the atomic coordinates being held constant at their room temperature values while the components of the $Cr^{3+}$ magnetic moments were refined. The cation coupling scheme found in $Fe_2(MoO_4)$ has the four crystallographically distinct cations divided into two pairs; each pair of cations aligns ferromagnetically but the two pairs are antiferromagnetically coupled. This arrangement gave a satisfactory account ($R_{mag}$ = 8.2%) of the magnetic scattering from $Cr_2(MoO_4)_3$ when the magnetic moments were constrained to lie in the ac plane. An alternative model in which the monoclinic symmetry was preserved by constraining the moments to lie along the *b* axis gave a less satisfactory fit. The final lattice parameters were $a$ = 15.5505(9), $b$ = 9.1667(7), $c$ = 18.1111(9), and $\beta$ = 125.40(1). The magnitude of the moment was refined to a value of 2.5$\mu_B$ although the large uncertainties in the atomic coordinates used in these calculations lead to a considerable uncertainty ($\sim\pm 0.2\mu_B$) in the value of the magnetic moment quoted here. A moment of 2.5 ± 0.2$\mu_B$ per cation is in reasonable agreement with that of 2.80 ± 0.08 found (*11*) previously for $Cr^{3+}$ in $LaCrO_3$. The magnetic ordering pattern of the cations in $Cr_2(MoO_4)_3$ is therefore the same as that found previously (*2*) in $Fe_2(MoO_4)_3$, except that in the latter case the spin direction lies along the *b* axis.

TABLE II

MO–O BOND LENGTHS IN $Cr_2(MoO_4)_3$[a]

| Bond | Length (Å) | Bond | Length (Å) |
|---|---|---|---|
| Mo(1)–O(20) | 1.60 | Mo(4)–O(21) | 1.72 |
| Mo(1)–O(9) | 1.70 | Mo(4)–O(18) | 1.73 |
| Mo(1)–O(7) | 1.82 | Mo(4)–O(14) | 1.80 |
| Mo(1)–O(12) | 1.84 | Mo(4)–O(16) | 1.81 |
| Mo(2)–O(3) | 1.72 | Mo(5)–O(17) | 1.65 |
| Mo(2)–O(13) | 1.72 | Mo(5)–O(24) | 1.73 |
| Mo(2)–O(2) | 1.73 | Mo(5)–O(19) | 1.77 |
| Mo(2)–O(4) | 1.88 | Mo(5)–O(23) | 1.85 |
| Mo(3)–O(15) | 1.72 | Mo(6)–O(22) | 1.67 |
| Mo(3)–O(6) | 1.74 | Mo(6)–O(11) | 1.69 |
| Mo(3)–O(5) | 1.75 | Mo(6)–O(1) | 1.85 |
| Mo(3)–O(8) | 1.80 | Mo(6)–O(10) | 1.86 |

[a] In a well determined structure, these would have a value of ca. 1.75 Å.

## Discussion

The results of our magnetic susceptibility and low-resolution neutron diffraction experiments indicate tht $Cr_2(MoO_4)_3$ is an L-type ferrimagnet with properties very similar to those of $Fe_2(MoO_4)_3$. Unfortunately Mossbauer spectroscopy, which characterizes the different cation sublattices better than any other technique (*1*), is not applicable to chromium and we are therefore unable to present a detailed analysis of the sublattice magnetizations. The susceptibility maximum of $Cr_2(MoO_4)_3$ is less pronounced than that of either $Fe_2(SO_4)_3$ or $Fe_2(MoO_4)_3$, suggesting that the cation environments are more nearly identical in $Cr_2(MoO_4)_3$ than in either of the iron compounds. This is not surprising in view of the strong preference for $Cr^{3+}$ for regular octahedral coordination. The dramatic increase in Curie temperature from 12 K in $Fe_2(MoO_4)_3$ to 42 K in $Cr_2(MoO_4)_3$ demonstrates the great strength of the $\pi$ superexchange in these systems. The unit-cell volume of $Cr_2(MoO_4)_3$ at 5 K (2104 Å$^3$) is 1.7% less than that of $Fe_2(MoO_4)_3$ (2140 Å$^3$) at the same temperature, implying a reduction of ~0.6% in the length of a typical superexchange pathway. This estimate agrees well with the percentage change in path length calculated from published values of the ionic radii of $Cr^{3+}$ and $Fe^{3+}$, and it implies that the strength of the magnetic coupling in this structure depends on cation size even more strongly than was predicted previously (*4*). The absence of $\sigma$ superexchange is a negligible factor compared to the decrease (~0.02 Å) in the cation radius which apparently brings about a large increase in the strength of the $\pi$ superexchange. Our results are consistent with those of Freund *et al.* (*12*) who used ENDOR techniques to demonstrate that the degree of oxygen-to-metal $\pi$ charge transfer increases by a factor of 3 on moving from $Fe^{3+}$ to $Cr^{3+}$ in an oxide environment. This increase in $\pi$ covalency explains the increase in Curie temperature on moving from $Fe_2(MoO_4)_3$ to $Cr_2(MoO_4)_3$. The change in magnetization direction can be attributed to either the slight structural changes which modify the dipole–dipole interactions in the material or to the small, second-order orbital component of the $Cr^{3+}$ magnetic moment.

Finally, we wish to draw attention to the imprecision that is found in the time-of-flight neutron refinement of $Cr_2(MoO_4)_3$. We believe that this arises primarily from the loss of resolution due to particle size broadening and does not necessarily reflect a limitation in the technique itself. It does, however, underline an important problem in high-resolution powder neutron diffraction; the enhanced resolution of the new generation of instruments will only realise its full potential if samples of high crystallinity can be prepared.

## Acknowledgments

We are grateful to SERC for a Research Studentship (W.T.A.H.) and the provision of neutron diffraction facilities. P.D.B. is grateful to the Central Electricity Generating Board and St. Catherine's College, Oxford, for a Research Fellowship.

## References

1. G. J. Long, G. Longworth, P. D. Battle, A. K. Cheetham, R. V. Thundathil, and D. Beveridge, *Inorg. Chem.* **18,** 624 (1979).
2. P. D. Battle, A. K. Cheetham, G. J. Long, and G. Longworth, *Inorg. Chem.* **21,** 4223 (1982).
3. L. Neel, *Ann. Phys. (Paris)* **3,** 137 (1948).
4. J. W. Culvahouse, *J. Magn. Magn. Mater.* **21,** 133 (1980).
5. C. Marcilly, P. Courty, and B. Delmon, *J. Amer. Ceram. Soc.* **53,** 56 (1970).
6. A. K. Cheetham and A. J. Skarnulis, *Anal. Chem.* **53,** 1060 (1981).
7. H. M. Rietveld, *J. Appl. Crystallogr.* **2,** 65 (1969).
8. R. B. Von Dreele, J. D. Jorgensen, and C. G. Windsor, *J. Appl. Crystallogr.* **15,** 581 (1982).
9. A. W. Sleight and L. H. Brixner, *J. Solid State Chem.* **7,** 172 (1973).
10. H. Y. Chen, *Mater. Res. Bull.* **14,** 1583 (1979).
11. B. C. Tofield and B. E. F. Fender, *J. Phys. Chem. Solids* **31,** 2741 (1970).
12. P. Freund, J. Owen, and B. F. Hahn, *J. Phys. C* **6,** L139 (1973).